

Journal Pre-proof

Bilayer chitosan-based patches for steroidal drug delivery on the oral mucosa

Elena Maria Varoni, Lina Altomare, Lorenzo Bonetti, Franca Viganò, Alessandro Scalia, Marcello Manfredi, Luigi De Nardo, Lia Rimondini, Andrea Cochis



PII: S1773-2247(24)00588-4

DOI: <https://doi.org/10.1016/j.jddst.2024.105919>

Reference: JDDST 105919

To appear in: *Journal of Drug Delivery Science and Technology*

Received Date: 27 March 2024

Revised Date: 25 June 2024

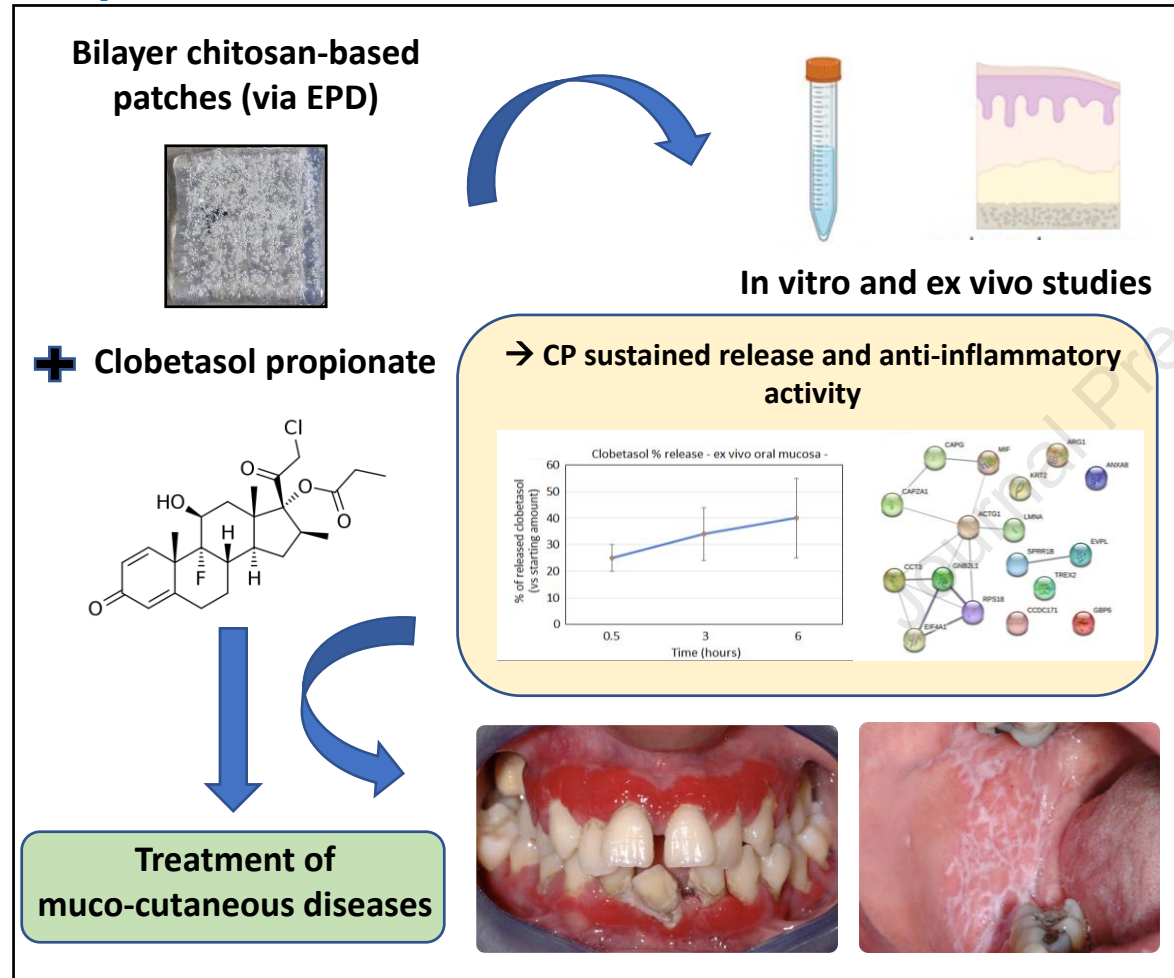
Accepted Date: 27 June 2024

Please cite this article as: E.M. Varoni, L. Altomare, L. Bonetti, F. Viganò, A. Scalia, M. Manfredi, L. De Nardo, L. Rimondini, A. Cochis, Bilayer chitosan-based patches for steroidal drug delivery on the oral mucosa, *Journal of Drug Delivery Science and Technology*, <https://doi.org/10.1016/j.jddst.2024.105919>.

This is a PDF file of an article that has undergone enhancements after acceptance, such as the addition of a cover page and metadata, and formatting for readability, but it is not yet the definitive version of record. This version will undergo additional copyediting, typesetting and review before it is published in its final form, but we are providing this version to give early visibility of the article. Please note that, during the production process, errors may be discovered which could affect the content, and all legal disclaimers that apply to the journal pertain.

© 2024 Published by Elsevier B.V.

Graphical Abstract



Research Highlights

- Highly lipophilic clobetasol propionate (CP) is successfully loaded on chitosan-based patches via electrophoretic deposition (EPD)
- Bilayer chitosan-based patches are promising mucoadhesive delivery systems for the oral cavity
- The presence of CP does not affect the mucoadhesive properties of chitosan-based patches
- CP, after the release from patches, maintains its biological immunosuppressive activity

1 **Bilayer chitosan-based patches for steroidal drug delivery on the oral mucosa**

2 Elena Maria Varoni^{1,2*}, Lina Altomare^{2,3}, Lorenzo Bonetti³, Franca Viganò¹, Alessandro Scalia⁴, Marcello
3 Manfredi⁵, Luigi De Nardo^{2,3}, Lia Rimondini^{4,*}, Andrea Cochis^{4,x}

4

5 ¹Dipartimento di Scienze Biomediche, Chirurgiche ed Odontoiatriche, Università degli Studi di Milano, Italy

6 ²National Interuniversity Consortium of Materials Science and Technology (INSTM), Florence, Italy

7 ³Department of Chemistry, Materials and Chemical Engineering "G. Natta", Politecnico di Milano

8 ⁴Department of Health Sciences, Center for Translational Research on Autoimmune and Allergic Diseases
9 CAAD, Università del Piemonte Orientale UPO, Italy

10 ⁵Department of Translational Medicine, Center for Translational Research on Autoimmune and Allergic
11 Diseases CAAD, Università del Piemonte Orientale UPO, Italy

12

13 * co-corresponding authors: elena.varoni@unimi.it ; lia.rimondini@med.uniupo.it

14 ^x co-shared last authors: lia.rimondini@med.uniupo.it ; andrea.cochis@med.uniupo.it

15

16 **Abstract word: 200**

17 **Word count: 4102**

18 **Reference count: 43**

19 **Figure/table counts: 5 figures; 2 tables**

20

21

22 **Abstract**

23 Clobetasol-17-propionate (CP) is the most potent, highly lipophilic topical corticosteroid, used for the
24 treatment of immune-mediated muco-cutaneous diseases. No commercial preparations are available for oral
25 cavity and galenic formulations are often ineffective due to the easy displacement by saliva and muscular
26 movements. Here, we developed and characterized a novel mucoadhesive patches for CP delivery on the oral
27 mucosa. Bilayer chitosan (CS)-based mucoadhesive patches (CS-CP) were produced via electrophoretic
28 deposition (EPD), and characterized for physical and biological properties. Bilayer CS-CP patches showed a
29 porous structure at the surface towards the oral mucosa (containing CP) and a more compact occlusive
30 backing layer (without CP). CS-CP patches displayed fast swelling ($301.6 \pm 0.8\%$) in PBS, while a sustained CP
31 release was observed over time, both *in vitro* in PBS and using an *ex vivo* model of porcine oral mucosa, with
32 about 40% of CP released after 6 h. CP did not affect the mucoadhesive properties of the patches. Through a
33 3D model of the oral mucosa, the patches' cytocompatibility and the activity of CP released in regulating
34 immune response-related pathways were evaluated. CS-based patches represent innovative biocompatible
35 biomedical devices for the oral mucosa, able of successfully loading highly lipophilic drugs, including CP.

36
37
38 **Keywords:** drug delivery, oral medicine, controlled release, mucocutaneous disorders, biomaterials

39

40 1. Introduction

41 Immune-mediated and autoimmune diseases involving the oral mucosa, such as recurrent aphthous
42 stomatitis (RAS), oral lichen planus (OLP), membrane mucous pemphigoid and pemphigus vulgaris, are often
43 associated with painful intraoral ulcers, which can impair the patient oral functions, reducing the quality of
44 life and sociability [1].

45 Being the etiopathogenesis still largely unknown, all these conditions require only symptomatic treatments,
46 and current management includes the use of immune-modulating drugs, particularly, topical steroids that
47 are the standard of care, aiming at reducing, locally, the chronic inflammation and the exaggerated immune
48 response [2]. Among topical steroids, clobetasol-17-propionate (CP) represents the most potent
49 corticosteroids (Europe: class IV) on the market, available only in form of creams and ointments for
50 dermatological topical application, due to its high lipophilicity. However, literature supports that CP is also
51 effective for the local treatment of oral immune-mediated and autoimmune diseases [3,4], despite the
52 absence of a standard formulation suitable for the oral cavity. To date, galenic formulations at 0.05% (w/w)
53 of CP in 4% hydroxyethylcellulose gel are usually prescribed to treat oral lesions, although showing poor
54 mucoadhesive properties with an easy displacement of the drug and a reduced clinical effectiveness. The
55 clinical success is affected by the difficult application of the drug on the oral mucosa, which is particularly
56 challenging due to the salivary flow, having washing effects, and to the muscular activity, which mechanically
57 displaces the drug during phonation and swallowing [5]. Moreover, the very high lipophilicity of CP can
58 further decrease the drug-to-mucosa contact time, while increasing the unpredictability of drug local
59 distribution, being the oral environment highly hydrophilic, instead. Strategies to improve the CP local effect,
60 by increasing mucoadhesion and the contact time, are currently under investigation with the final aim of
61 obtaining a more effective topical drug delivery system, thus reducing the need of systemic
62 immunosuppressive therapies, often correlated with systemic adverse effects.

63 The ideal properties of a drug delivery system for the oral mucosa include high mucoadhesion and
64 unidirectional drug release toward epithelial tissue, prolonging the mucosal exposure to the drug, thus
65 increasing drug permeation throughout epithelial layers [6]. From a mechanical point of view, the device

66 should also show appropriate mechanical flexibility to support any movement within the oral cavity and it
67 should be compatible with the salivary environment that is highly hydrophilic and with an average pH of 6.7
68 (range 6.2 -7.6) [7]. One of the most challenging aspects, considering that CP is very lipophilic, is related to
69 the need of loading the lipophilic drug into the mucoadhesive system and to release it towards the oral
70 mucosa, into an aqueous environment.

71 Drug delivery systems for steroidal drugs in the oral mucosa have included polymeric gels, mouthwashes,
72 sprays, particulates, films and patches [8–12], although only few reports focused on CP [13–16]. Low drug
73 loading efficiency, initial burst release, and the possibility of drug expulsion during storage were the main
74 drawbacks. Bilayered buccal patches [13] have been proposed, based on polyvinylpyrrolidone (PVP) and
75 polycaprolactone (PCL), synthetic polymers that require the need of toxic solvents for the preparation, high
76 hydrophobicity and a lack of antimicrobial activity [17,18]. Recently, the Rivelin®- CLO bilayer patches, which
77 are composed of synthetic polymers, i.e. PVP and Eudragit RS100 for the mucoadhesive electrospun
78 nanofibers loaded with CP and PCL for the occlusive backing layer, were tested in OLP patients in randomized
79 placebo-controlled clinical trial, showing promising results [19].

80 Here, we propose novel bilayer mucoadhesive oral patches based on chitosan (CS), a natural polymer derived
81 from shrimps, to propose an innovative drug delivery system, highly biocompatible and biodegradable,
82 prepared without the need of synthetic polymers or toxic solvents. CS is a biodegradable polysaccharide with
83 intrinsic bio-adhesive [20], anti-microbial and wound healing properties [21]. To date, CS-based buccal
84 patches were obtained by solvent casting technique or electrophoretic deposition (EPD), loading different
85 drugs, such as verapamil, carvedilol or lidocaine, adding additives to improve biomechanical properties, such
86 as polyvinylpyrrolidone (PVP), methylcellulose and pectin [22–25], or functionalizing CS with catechol groups
87 [26].

88 The aim of this study was to synthesize and characterize innovative CS-based bilayer buccal patches, loaded
89 with CP, via EPD. The patches displayed a bilayer design with an occlusive backing side, not loaded with the
90 drug (towards the oral environment), and a CP-loaded side (towards the mucosa), to promote the
91 unidirectional release of the drug to the target site. The patches were characterized from a morphological

92 and physical point of view, then the release of CP in physiological solution was assessed. An *ex vivo* model of
93 porcine oral mucosa was used to test the mucoadhesive properties of the patches and assess CP diffusion
94 throughout the epithelial layers. Finally, an *in vitro* 3D model of human oral mucosa was used to verify the
95 patches' cytocompatibility and, via proteomics, the bioactivity of the CP released locally.

96

Journal Pre-proof

97 **2. Materials and Methods**

98 **2.1 EPD of bilayer CS-CP patches**

99 All reagents were provided by Sigma-Aldrich® (St. Louis, Missouri). CP (1g L^{-1} , molecular weight = 466.97) was
100 added to a CS (1g L^{-1} , CS medium molecular weight, 75-85 % deacetylation degree) solution prepared with
101 30% water + 70% ethanol, adjusted to a pH = 4.8 with acetic acid. Titanium plates (Ti, grade 2) were used as
102 cathode in an electrophoretic deposition (EPD) process and two graphite rods used as anodes. The EPD
103 conditions were optimized to obtain bilayer CS-CP patches: EPD was carried out in potentiostatic mode by
104 applying a square waveform (100 - 75 V, duty cycle (DC) = 0.17, $t = 5$ min) using a power supply (Keithley
105 2425, Keithley Instruments). The CP concentration in the bath and the EPD conditions were based on previous
106 data about CP loading on monolayer CS-based EPD patches, reported elsewhere [27]. Bilayer patches, in
107 particular, were obtained by a double step EPD deposition: a first deposition was deposited starting from a
108 solution bath, as reported above, containing only CS (backing layer) and, after drying ($T = 37\text{ }^{\circ}\text{C}$ for 1.5 h), a
109 second layer was deposited starting the same CS solution with the addition of CP, namely CS-CP (test
110 samples). In case of control samples, the second deposition included only the CS solution (without the
111 addition of CP). The obtained bilayer patches were then oven dried ($T = 37\text{ }^{\circ}\text{C}$ for 24 h) and peeled off from
112 the cathode.

113 **2.2 Morphological surface analysis**

114 The morphology of the bilayer porous dried scaffolds was evaluated with optical microscopy and by means
115 of a Scanning Electron Microscope (SEM) at 10 kV (SEM, Stereoscan 360, Cambridge). Pore diameter was
116 measured in triplicate each type of sample, by means of ImageJ software, by analyzing at least 10 pores per
117 image.

118 **2.3 Swelling properties**

119 The water uptake test was performed to investigate swelling behavior of CP-loaded CS patches. The swelling
120 properties of the patches were studied by immersing them in 1 ml of Phosphate Buffer Solution (PBS)
121 (pH=7.4) at room temperature. The dried patches ($1 \times 1\text{ cm}^2$) weighed (W_0). At considered time points (up to
122 8 different time points), patches were removed from the solution and carefully dried using filter paper; free

123 water was removed, leaving only the interstitial water trapped in the polymer network. The specimens were
124 then weighed (W_t) and put back into the solution. At each time point, the percentage of water uptake was
125 calculated using the following equation:

$$126 \quad (W_t - W_0) / W_0 \times 100$$

127 W_t = the weight of the patch at time t

128 W_0 = the weight of the patch at time zero

129 **2.4 CP loading**

130 CP concentration in CS patches was investigated using liquid chromatography mass spectrometry (LC-MS).
131 The patches ($1 \times 1 \text{ cm}^2$) were weighed and then dissolved in 1 mL of acetic acid (10%v/v) and 200 μL of
132 ethanol. The solution was then collected and analyzed by LC-MS. LC-MS analyses were performed using a
133 mass spectrometer Orbitrap Q-Exactive Plus coupled with an Ultra High-Performance Liquid Chromatography
134 (UHPLC) Vanquish (Thermo Fisher, Milano).

135 **2.5 CP in vitro release into physiological solutions**

136 CP concentration released from CS patches ($1 \times 1 \text{ cm}^2$) was analyzed by liquid chromatography mass
137 spectrometry (LC-MS). CP release kinetics was performed in a dissolution medium (0.5M PBS and 0.5%
138 sodium dodecyl sulphate, pH 6.8) at 37 °C: each patch was incubated in 1 ml of solution, and fixed vertically
139 in 2 ml tubes in agitation (100 rpm, 37°C), thus allowing CP release from the patch. The solution was collected
140 at 5, 10, 20, 40 and 60 min and analyzed by LC-MS, using a mass spectrometer Orbitrap Q-Exactive Plus
141 coupled with an Ultra High-Performance Liquid Chromatography (UHPLC) Vanquish (Thermo Fisher, Milano).

142 **2.6 CP release using an ex vivo model of porcine oral mucosa**

143 Samples of porcine oral mucosa were surgically resected from whole porcine cheeks (kindly provided by Prof.
144 Elena Grossini, Laboratory of Physiology – University of Piemonte Orientale), then wetted with PBS solution
145 at physiological conditions. The porcine oral mucosa specimens were prepared with standard dimensions, as
146 squares (2 cm side and 5 mm thickness), then maintained in DMEM/F12 medium at 37°C. Patches were
147 applied, with gentle pressure, onto mucosa samples at the air-liquid interface and allowed to spontaneously
148 release CP for 0.5, 3 and 6 h. At each time-point, mucosa samples were separated from patches, mechanically

149 homogenized and the released CP was analyzed by LC-MS, using a mass spectrometer Orbitrap Q-Exactive
150 Plus coupled with an Ultra High-Performance Liquid Chromatography (UHPLC) Vanquish (Thermo Fisher,
151 Milano).

152 **2.7 Patches' mucoadhesion using an ex vivo model of porcine oral mucosa**

153 A tack-test was performed using the modular compact Anton Paar MCR302 rheometer and porcine oral
154 mucosa as standard mucosal substrate for testing mucoadhesion, in accordance with the ASTM F2258
155 standard. The porcine oral mucosa specimens (prepared as squares of 10 mm-side and 5mm-thickness; n=5
156 per sample type) were deeply washed with PBS and frozen at -20°C for the further mechanical analyses. After
157 being re-equilibrated at room temperature (RT), porcine buccal mucosa pieces were attached to the lower
158 disposable plate of the device. Wet patches (CS or CS-CP) were similarly fixed on the upper disposable plate
159 of the instrument ($\phi = 25$ mm). Mucosa and patches were placed in contact: a compressive preload of 1 N
160 force was applied for 10 s. Then, the upper plate was moved upwards at a constant speed of 50 mm/min
161 until detachment. The release pressure ($\sigma_{adh} = F/S$; where F is the Force of detachment and S is the contact
162 area) and the muco-adhesion work ($W_{adh} = AUC$; where AUC is the area under the σ_{adh} – displacement curve
163 calculated using OriginPro software) were measured as previously reported [28,29].

164 **2.8 Patches' cytocompatibility using a 3D model of human oral mucosa**

165 CP-loaded patch toxicity was investigated *in vitro* by analysing the metabolic activity of the oral mucosa
166 tissue, after a 24 h-direct contact with the patches. Accordingly, wet bilayer patches (both CS-CP and CS)
167 were gently seeded in direct contact with a 3D model of human oral mucosa (SkinEthic HOE, from EPISKIN,
168 Lyon, France), allowed to adhere for 2 h and then maintained for 24h at 37°C at 5% CO₂, using the
169 maintenance medium as provided by the manufacturer CS patches were used as control considering previous
170 literature supporting the safety both *in vitro* and *in vivo* of this biomaterial [30]. Metabolic activity of cells
171 contained in the oral mucosa was further evaluated by using the colorimetric/fluorometric assay Alamar Blue
172 (Thermo Fisher, Waltham, Massachusetts, USA), following manufacturer's instruction. Briefly, the Alamar
173 blue solution was diluted (10%) and put in contact with the 3D model of oral mucosa for 3h, in the dark. Then,
174 100 μ l of solution have been collected, spotted in a black plate and fluorescent signals were evaluated with a

175 spectrophotometer (Spark multimode microplate reader, Tecan, Männedorf, Svizzera) excitation wavelength
176 530 nm, fluorescence emission reading 590 nm. Results are reported as Relative Fluorescence Units (RFU).

177 **2.9 Proteomics analysis to test biological activity of released CP on a 3D model of human oral mucosa**

178 The biological effect of CP released from the patch was assessed by proteomics analysis on the tissue in direct
179 contact with the patches. Wet specimens (both CS-CP and CS) were gently seeded in direct contact with the
180 3D model of human oral mucosa (SkinEthic HOE, from EPISKIN, Lyon, France), allowed to adhere for 2 h and
181 then maintained for 24h at 37°C at 5% CO₂ using the maintenance medium as provided by the manufacturer.
182 Tissue samples were lysed with RIPA buffer and denatured with TFE (Sigma-Aldrich Inc., St. Louis, MO, USA)
183 and then subjected to reduction with DTT 200 mM, to alkylation with IAM 200mM and to complete protein
184 digestion with 2 µg of Trypsin (Sigma-Aldrich Inc., St. Louis, MO, USA). The peptide digests were desalted on
185 the Discovery® DSC-18 solid phase extraction (SPE) 96-well plate (25 mg/well) (Sigma-Aldrich Inc., St. Louis,
186 MO, USA). After the desalting process, the sample was vacuum-evaporated and reconstituted in mobile
187 phase for the analysis [31]. The digested peptides were analyzed with a UHPLC Vanquish system (Thermo
188 Scientific, Rodano, Italy) coupled with an Orbitrap Q-Exactive Plus (Thermo Scientific, Rodano, Italy). Peptides
189 were separated by a reverse phase column (Accucore™ RP-MS 100 x 2.1 mm, particle size 2.6 µm). The
190 column was maintained at a constant temperature of 40 °C at a flow rate of 0.200 mL/min. Mobile phase A
191 and B were water and acetonitrile respectively, both acidified with 0.1% formic acid. The analysis was
192 performed using the following gradient: 0-5 min from 2% to 5% B; 5-55 min from 5% to 30% B; 55-61 from
193 30% to 90% B and hold for 1 min, at 62.1 min the percentage of B was set to the initial condition of the run
194 at 2% and hold for about 8 min in order to re-equilibrate the column, for a total run time of 70 min. The Mass
195 spectrometry analysis was performed in positive ion mode. The ESI source was used with a voltage of 2.8 kV.
196 The capillary temperature, sheath gas flow, auxiliary gas and spare gas flow were set at 325 °C, 45 arb, 10 arb
197 and 2 respectively. S-lens was set at 70 rf. For the acquisition of spectra, a data-dependent (ddMS2) top 10
198 scan mode was used. Survey full-scan MS spectra (mass range m/z 381 to 1581) were acquired with
199 resolution R = 70,000 and AGC target 3x10⁶. MS/MS fragmentation was performed using high-energy c-trap
200 dissociation (HCD) with resolution R = 35,000 and AGC target 1x10⁶. The normalized collision energy (NCE)

201 was set to 30. The injection volume was 3 μ L. The mass spectra analysis was carried out using MaxQuant
202 software (version 1.6.14). MaxQuant parameters were set as follow: trypsin was selected for enzyme
203 specificity; the search parameters were fixed to an initial precursor ion tolerance of 10 ppm and MS/MS
204 tolerance at 20 ppm; as fixed modification, carbamidomethylation was set, whereas oxidation was set as
205 variable modification. The maximum missed cleavages were set to 2. Andromeda search engine searched the
206 spectra in MaxQuant against the Uniprot_CP_Human_2018 sequence database. Label free quantification was
207 performed including a match between runs option with the following parameters: protein and peptide false
208 discovery rate was set to 0.01; the quantification was based on the extracted ion chromatograms, with a
209 minimum ratio count of 1; the minimum required peptide length was set to 7 aminoacids. Statistical analysis
210 was performed using MaxQuant software (version 1.6.14) and MetaboAnalyst software
211 (<https://www.metaboanalyst.ca/>) [32].

212 **2.10 Statistical analysis**

213 Experiments were performed in triplicate. Results were statistically analyzed using the SPSS software (v.20.0,
214 IBM, USA). Groups were compared by the one-way ANOVA using the Tukey's test as a post-hoc analysis.
215 Significant differences were established at $p < 0.05$.

216

217

218

219 **3. Results**

220 **3.1 Morphological surface analysis**

221 CS-CP patches were successfully obtained (Figure 1 A and B) via EPD. At optical microscopy, bilayer CS-CP
222 patches showed a complex random macroporosity with a pore dimension similar to bilayer CS patches (Figure
223 1 C and D).

224 SEM images showed dried bilayer CS patches with a more compact structure, with the minimum presence of
225 isolated roughness (Figure 2 A and B), while bilayer CS-CP patches displayed higher random microporosity
226 (Figure 2 C and D). The two deposited layers were indistinguishable (Figure 2 D), and appeared stably
227 adhering each other, also after immersion in PBS (data not shown). Moreover, bilayer CS-CP patches also
228 displayed the presence of surface microspheres as observed at a lower magnification, ascribable to
229 superficial CP deposits (Figure 2 E). The latter were no more visible after washing with PBS and ethanol, and
230 a homogeneous and regular microporosity was instead detectable (Figure 2 F). Pore dimensions of CS-CP
231 patches were further characterized using SEM image analysis and showed a mean pore size of $3.0 \pm 0.7 \mu\text{m}$
232 in the dried state.

233 **3.2 Swelling properties**

234 The swelling data in PBS (pH=7.4) comparing CS patches and CS-CP patches are shown in Figures 3. Both
235 patches displayed a similar swelling kinetics with fast swelling after immersion in the solution up to a stable
236 plateau achieved after 2 h. The mean swelling rate was of $346.0 \pm 0.3\%$ for CS patches, while of $301.6 \pm 0.8\%$
237 for CS-CP patches, with no statistically significant difference.

238 **3.3 CP loading and release kinetics**

239 The LC-MS data showed that CP was successfully loaded in the patches at a concentration $0.9 \pm 0.2 \mu\text{g}/\text{mg}$ of
240 patch.

241 At *in vitro* release test, using $1 \times 1 \text{ cm}^2$ patches immersed in 1 mL of PBS, a sustained release over the time
242 could be observed. The amount of drug released was about $1.2 \pm 0.8 \mu\text{g}/\text{mL}$ of solution, as achieved after 40
243 min and corresponding to >30% of the loaded CP ($33.0 \pm 9.5\%$). Figure 3A and B summarizes the release
244 profile of CP from CS-CP patches. The sustained release was confirmed at *ex vivo* release test, using porcine

245 oral mucosa, with about 40% of the loaded CP released within the tissue after 6 h; the released drug amount
246 was of $1.3 \pm 0.7 \mu\text{g/mL}$ (Figure 4 C and D).

247 **3.4 Mucoadhesion using ex vivo model of porcine oral mucosa**

248 No significant differences were observed between CS and CS-CP for both release pressure at detachment
249 ($557 \pm 213 \text{ Pa}$ and $448 \pm 8 \text{ Pa}$, respectively) and W_{adh} ($745 \pm 126 \text{ Pa}\cdot\text{mm}$ and $699 \pm 128 \text{ Pa}\cdot\text{mm}$, respectively),
250 and the drug did not affect the mucoadhesive behavior of CS (Table 2).

251 **3.5 Patches' cytocompatibility using a 3D model of human oral mucosa**

252 The 3D model of human oral mucosa was cultivated for 24 h in direct contact with the patches. The
253 cytocompatibility results are shown in the Figure 5A: no significant differences were observed between CS
254 and CS-CP in terms of metabolic activity, after 24 h of contact with the oral mucosa model ($p > 0.05$), thus
255 suggesting a favorable cells-friendly behavior of the patches under investigation.

256 **3.6 Proteomics analysis to test biological activity of released CP on a 3D model of human oral mucosa**

257 The analysis of protein extracted from the oral mucosa models in contact with CS or CS-CP patches revealed
258 the presence of 263 protein. Among them, seven were down-regulated and ten up-regulated, as described
259 in Figure 5 C and D, and the map of their interconnection showed consistency in regulating immune response-
260 related pathways, including macrophage migration inhibitory factor (MIF) downregulation and GBP6 and
261 RACK1 up-regulation as shown in Figure 5B.

262

263 **4. Discussion**

264 Oral mucosa can be affected by painful lesions, which can be ascribed to immune-mediated or auto-immune
265 disorders that severely impact the patient's quality of life, impeding patient's nutrition because of difficulty
266 in chewing and in taking acidic foods, such as some fruits and vegetables.

267 These lesions are usually managed by topical corticosteroids, although a "gold standard" drug delivery system
268 for the oral mucosa is still lacking. The *in situ*-controlled release kinetics of drugs, on the oral mucosa, is
269 particularly challenging because of the moist mucosal surfaces, salivary flow and muscular forces, which
270 easily displace the delivery system and the loaded drug, decreasing the drug residence time that is pivotal
271 for the topical efficacy of a compound. In an attempt to address these issues, previous works proposed new
272 delivery systems for CP [13–15,19]. In a previous work, we optimized the EPD conditions to obtain monolayer
273 CS patches able to effectively incorporate CP [27]. Here, we further developed and characterized a bilayer
274 mucoadhesive CS patch for CP delivery to the oral mucosa, having an occlusive side toward the oral
275 environment and the opposite side, towards the oral mucosa, containing CP, in order to obtain the
276 unidirectional release of the drug, thus representing a significative improvement in comparison to the
277 previous monolayer model.

278 This works confirms EPD as a simple, low-cost and fast approach to incorporate water insoluble agents into
279 CS matrix; EPD is available at industrial scale for industrial calcium phosphate coatings on metal prosthesis.
280 The amount of loaded CP (0.9 µg/mg) was comparable with the amount of drug contained in the galenic
281 formulation used in the clinical setting (0.5 µg/mg). The presence of CP within the bilayer CS patches resulted
282 in the presence of micropores, more evident than in our previous work on monolayer CS-CP patches [27].

283 Several approaches have been reported in the literature for the fabrication of mucoadhesive drug delivery
284 systems for the oral mucosa, such as gels, tablets, films, and patches [33,34]. Oral films and patches usually
285 display superior properties compared to other adhesive systems, being flexible and soft, yet resistant to the
286 mechanical stresses acting on the oral cavity [35]. In this panorama, non-traditional fabrication approaches
287 like EPD and electrospinning have attracted significant attention due to the possibility to one-pot fabricate
288 drug-loaded patches with superior mucoadhesive properties [36]. Both the techniques have been reported

289 for the fabrication of CS patches [27,33,37,38], even if it is difficult to compare their adhesive performances
290 mainly due to the lack of mucoadhesion tests in most of these studies. Furthermore, the comparison of the
291 drug loading/release is also non-trivial due to the different drugs and different test conditions (*in vitro*, *in*
292 *vivo*, *ex vivo*) used. However, such approaches should be preferred over traditional ones given the possibility
293 they offer to fabricate patches with a high surface-area-to-volume ratio and to load drugs directly in the
294 fabrication process, in a straightforward, cost-effective, and tunable way.

295 CS-CP samples showed a slightly ($p > 0.05$) lower swelling rate compared to bilayer CS patches. Although not
296 significant, such a difference in the swelling values could be attributed to the lipophilic nature of CP, which
297 could act reducing the overall swelling capacity of the loaded patch. Nevertheless, CS-CP patches preserved
298 satisfactory swelling levels, a crucial aspect for bio-adhesion. Mucoadhesive patches, indeed, are required to
299 display a rapid hydration and subsequent gelation of the polymers on the moist oral mucosal surface, leading
300 to physical and chemical interactions at the biomaterial–mucus interface. Besides hydrogen bonding and
301 hydrophobic interactions, CS can bind mucin mainly via electrostatic interactions, involving positively charged
302 amino groups of CS and negatively charged sialic acid residues of mucin [39,40]. Overall, the presence of CP
303 did not significantly affect mucoadhesive properties. Adequate mucoadhesion is crucial to ensure the
304 prolonged presence of the patches at the intended location that, in turn, leads to a constant release of the
305 drug at the lesion's site.

306 Considering the release profile, the CS-CP patches slowly released the drug in a sustained manner over 6 h
307 as confirmed by the swine *ex-vivo* model; however, it must be considered that, despite the notable
308 correspondence in terms of permeability between the pig and human oral mucosa [41], the use of a static
309 protocol may represent a limitation in the interpretation of the data. Therefore, for future insights the use
310 of perfusion model such as the modified Franz cell model [42] can be considered to confirm the results in a
311 more physiologically relevant model. By now, we can consider our results in line with previous literature such
312 as Colley *et al.*, who developed patches made of CP-loaded PVP and a PCL backing layer [13].

313 The cytocompatibility data supported the safety of the CP-loaded patches on the 3D human oral mucosa
314 model, after 24 h from the contact. These results match with the ones obtained by Kumar *et al.* and

315 Panonnummal *et al.* [43,44], who tested CP activity on human monocytes (THP-1) and human keratinocytes
316 (HACAT) cell lines. Their study demonstrated CP safety at higher concentrations (62.5 and 43.0 µg/mL,
317 respectively) than the one released by the patches here developed (1.2 ± 0.8 µg/mL).

318 The comparative analysis between the proteins extracted from the 3D model of human oral mucosa in
319 contact with CS patches (used as a control) *versus* CS-CP patches (test samples), performed by proteomics,
320 showed 17 proteins up- or down-regulated by the released CP within the mucosal tissue. Skin equivalents
321 represent a suitable model to study the biological effect of the released drug because the relevance of the
322 results does not strictly depend on the delivery system as demonstrated by Said *et al.* [14], dealing with the
323 release of corticosteroids. However, some elements of the living tissue influencing the drug diffusion, such
324 as the mucus and saliva keeping moist the epithelial surface, are effectively missing in the skin equivalents
325 therefore representing a limitation of the model [45]. Here, the most up-regulated protein was Guanylate-
326 binding proteins (GBP-6): GBPs are factors involved in the defense against cellular pathogens and
327 inflammation [46]. A further up-regulated protein was the Receptor for activated C kinase 1 (RACK1), a
328 scaffolding protein involved in the recruitment, assembly and regulation of a variety of signaling molecules,
329 including those related to immune response [47]. RACK1, in particular, represents an important target for
330 steroids [48]. Further overexpressed proteins include the Three prime repair exonuclease 2 (TREX2), the
331 Macrophage-capping protein (CAP-G) and other proteins involved in keratinization, like Keratin type II (K22E)
332 and Small Proline-Rich 1 (SPR1B). Among the downregulated proteins, the most biologically important one
333 was represented by the Macrophage migration inhibitory factor (MIF), a pro-inflammatory cytokine involved
334 in the innate immune response to bacterial pathogens *in vivo*, acting as mediator in regulating the function
335 of macrophages in host defense [49]. This protein also counteracts the anti-inflammatory activity of
336 glucocorticoids [49]; therefore, its down-regulation, related to CP *in situ* release, confirms the maintenance
337 of bioactivity of the drug from the CS-CP patches.

338

339 5. Conclusions

340 CP, a highly lipophilic drug, can be successfully loaded in double layer CS-based patches via EPD, a simple,
341 low-cost and fast fabrication technique. Bilayer CS-CP patches showed fast swelling, mucoadhesive
342 properties and a porous structure at the surface towards the oral mucosa (containing CP). A sustained CP
343 release was observed over time both *in vitro* in PBS and using an *ex vivo* model of porcine oral mucosa.
344 Patches showed an overall biocompatibility when directly put in contact with a 3D model of human oral
345 mucosa, and the released CP within the tissue maintained its anti-inflammatory effects *in situ*. Our study
346 demonstrated the possibility of obtaining bilayer mucoadhesive patches, loaded with CP and based on the
347 natural polymer CS, highly biocompatible and biodegradable, resulting in a promising topical therapeutic
348 strategy for the treatment of immune-mediated oral diseases.

349

350 **Acknowledgments**

351 The Authors are grateful to Prof. Elena Grossini, Laboratory of Physiology – University of Piemonte Orientale
352 for kindly providing the porcine oral mucosa for the *ex vivo* tests.

353 **Authors contributions**

354 All authors gave their final approval and agree to be accountable for all aspects of the work. EV contributed
355 to conception and design, drafted the manuscript; LA, LDN, LR contributed to design, critically revised the
356 manuscript; LB, FV, MM contributed to acquisition, analysis, and interpretation, critically revised the
357 manuscript; AS contributed to acquisition, analysis, and interpretation, drafted the manuscript; AC
358 contributed to contributed to acquisition, analysis, and interpretation, drafted the manuscript.

359 **Declaration of Conflicting Interests**

360 The authors declared no potential conflicts of interest with respect to the research, authorship, and/or
361 publication of this article.

362 **Funding**

363 The authors received no financial support for the research, authorship, and/or publication of this article,
364 besides funding from their own Institution.

365 **Data availability**

366 Data will be made available on request.

367

368

369 **References**

370

- 371 [1] P. Wiriyakijja, S. Porter, S. Fedele, T. Hodgson, R. McMillan, M. Shephard, R.N. Riordain, Health-
 372 Related Quality of Life and Its Associated Predictors in Patients with Oral Lichen Planus: A Cross-
 373 Sectional Study, *Int. Dent. J.* 71 (2021) 140–152. <https://doi.org/10.1111/idj.12607>.
- 374 [2] M. Oren-Shabtai, N. Kremer, M. Lapidoth, E. Sharon, L. Atzmony, A. Nosrati, E. Hodak, D. Mimouni, A.
 375 Levi, Treatment of Bullous Pemphigoid in People Aged 80 Years and Older: A Systematic Review of the
 376 Literature, *Drugs Aging* 38 (2021) 125–136. <https://doi.org/10.1007/s40266-020-00823-5>.
- 377 [3] G. Lodi, M. Manfredi, V. Mercadante, R. Murphy, M. Carrozzo, Interventions for treating oral lichen
 378 planus: corticosteroid therapies, *Cochrane Database Syst. Rev.* (2020).
 379 <https://doi.org/10.1002/14651858.CD001168.pub3>.
- 380 [4] A. Buonavoglia, P. Leone, R. Dammacco, G. Di Lernia, M. Petruzzi, D. Bonamonte, A. Vacca, V.
 381 Racanelli, F. Dammacco, Pemphigus and mucous membrane pemphigoid: An update from diagnosis to
 382 therapy, *Autoimmun. Rev.* 18 (2019) 349–358. <https://doi.org/10.1016/j.autrev.2019.02.005>.
- 383 [5] S. Agarwal, S. Aggarwal, Mucoadhesive polymeric platform for drug delivery; a comprehensive review,
 384 *Curr. Drug Deliv.* 12 (2015) 139–156. <https://doi.org/10.2174/1567201811666140924124722>.
- 385 [6] C.B. Fox, J. Kim, L.V. Le, C.L. Nemeth, H.D. Chirra, T.A. Desai, Micro/nanofabricated Platforms for Oral
 386 Drug Delivery, *J. Control. Release Off. J. Control. Release Soc.* 219 (2015) 431–444.
 387 <https://doi.org/10.1016/j.jconrel.2015.07.033>.
- 388 [7] S. Baliga, S. Muglikar, R. Kale, Salivary pH: A diagnostic biomarker, *J. Indian Soc. Periodontol.* 17 (2013)
 389 461–465. <https://doi.org/10.4103/0972-124X.118317>.
- 390 [8] R. Kumria, A.B. Nair, G. Goomber, S. Gupta, Buccal films of prednisolone with enhanced
 391 bioavailability, *Drug Deliv.* 23 (2016) 471–478. <https://doi.org/10.3109/10717544.2014.920058>.
- 392 [9] H.O. Ammar, M.M. Ghorab, A.A. Mahmoud, H.I. Shahin, Design and In Vitro/In Vivo Evaluation of
 393 Ultra-Thin Mucoadhesive Buccal Film Containing Fluticasone Propionate, *AAPS PharmSciTech* 18
 394 (2017) 93–103. <https://doi.org/10.1208/s12249-016-0496-0>.
- 395 [10] C. Zhang, Y. Liu, W. Li, P. Gao, D. Xiang, X. Ren, D. Liu, Mucoadhesive buccal film containing ornidazole
 396 and dexamethasone for oral ulcers: in vitro and in vivo studies, *Pharm. Dev. Technol.* 24 (2019) 118–
 397 126. <https://doi.org/10.1080/10837450.2018.1428814>.
- 398 [11] X. Guo, T. Zhu, X. Yu, X. Yi, L. Li, X. Qu, Z. Zhang, Y. Hao, W. Wang, Betamethasone-loaded dissolvable
 399 microneedle patch for oral ulcer treatment, *Colloids Surf. B Biointerfaces* 222 (2023) 113100.
 400 <https://doi.org/10.1016/j.colsurfb.2022.113100>.
- 401 [12] S. Hu, X. Pei, L. Duan, Z. Zhu, Y. Liu, J. Chen, T. Chen, P. Ji, Q. Wan, J. Wang, A mussel-inspired film for
 402 adhesion to wet buccal tissue and efficient buccal drug delivery, *Nat. Commun.* 12 (2021) 1689.
 403 <https://doi.org/10.1038/s41467-021-21989-5>.
- 404 [13] H.E. Colley, Z. Said, M.E. Santocildes-Romero, S.R. Baker, K. D’Apice, J. Hansen, L.S. Madsen, M.H.
 405 Thornhill, P.V. Hatton, C. Murdoch, Pre-clinical evaluation of novel mucoadhesive bilayer patches for
 406 local delivery of clobetasol-17-propionate to the oral mucosa, *Biomaterials* 178 (2018) 134–146.
 407 <https://doi.org/10.1016/j.biomaterials.2018.06.009>.
- 408 [14] Z. Said, C. Murdoch, J. Hansen, L. Siim Madsen, H.E. Colley, Corticosteroid delivery using oral mucosa
 409 equivalents for the treatment of inflammatory mucosal diseases, *Eur. J. Oral Sci.* 129 (2021) e12761.
 410 <https://doi.org/10.1111/eos.12761>.
- 411 [15] G. Campisi, G. Giandalia, V. De Caro, C. Di Liberto, P. Aricò, L.I. Giannola, A new delivery system of
 412 clobetasol-17-propionate (lipid-loaded microspheres 0.025%) compared with a conventional
 413 formulation (lipophilic ointment in a hydrophilic phase 0.025%) in topical treatment of
 414 atrophic/erosive oral lichen planus. A Phase IV, randomized, observer-blinded, parallel group clinical
 415 trial, *Br. J. Dermatol.* 150 (2004) 984–990. <https://doi.org/10.1111/j.1365-2133.2004.05943.x>.
- 416 [16] G.F. Racaniello, M. Pistone, C. Meazzini, A. Lopodota, I. Arduino, R. Rizzi, A. Lopalco, U.M. Musazzi, F.
 417 Cilurzo, N. Denora, 3D printed mucoadhesive orodispersible films manufactured by direct powder

- 418 extrusion for personalized clobetasol propionate based paediatric therapies, *Int. J. Pharm.* 643 (2023)
 419 123214. <https://doi.org/10.1016/j.ijpharm.2023.123214>.
- 420 [17] M.S.B. Reddy, D. Ponnamma, R. Choudhary, K.K. Sadasivuni, A Comparative Review of Natural and
 421 Synthetic Biopolymer Composite Scaffolds, *Polymers* 13 (2021) 1105.
 422 <https://doi.org/10.3390/polym13071105>.
- 423 [18] L. Dobrzanski, A. Hudecki, G. Chladek, W. Król, A. Mertas, Biodegradable and antimicrobial
 424 polycaprolactone nanofibers with and without silver precipitates, *Arch. Mater. Sci. Eng.* 76 (2015) 5–
 425 26.
- 426 [19] M.T. Brennan, L.S. Madsen, D.P. Saunders, J.J. Napenas, C. McCreary, R. Ni Riordain, A.M.L. Pedersen,
 427 S. Fedele, R.J. Cook, R. Abdelsayed, M.T. Llopiz, V. Sankar, K. Ryan, D.A. Culton, Y. Akhlef, F. Castillo, I.
 428 Fernandez, S. Jurge, A.R. Kerr, C. McDuffie, T. McGaw, A. Mighell, T.P. Sollecito, T. Schlieve, M.
 429 Carrozzo, A. Papas, T. Bengtsson, I. Al-Hashimi, L. Burke, N.W. Burkhart, S. Culshaw, B. Desai, J.
 430 Hansen, P. Jensen, T. Menné, P.B. Patel, M. Thornhill, N. Treister, T. Ruzicka, Efficacy and safety of a
 431 novel mucoadhesive clobetasol patch for treatment of erosive oral lichen planus: A phase 2
 432 randomized clinical trial, *J. Oral Pathol. Med.* 51 (2022) 86–97. <https://doi.org/10.1111/jop.13270>.
- 433 [20] I.A. Sogias, A.C. Williams, V.V. Khutoryanskiy, Why is Chitosan Mucoadhesive?, *Biomacromolecules* 9
 434 (2008) 1837–1842. <https://doi.org/10.1021/bm800276d>.
- 435 [21] A. Francesko, T. Tzanov, Chitin, chitosan and derivatives for wound healing and tissue engineering,
 436 *Adv. Biochem. Eng. Biotechnol.* 125 (2011) 1–27. https://doi.org/10.1007/10_2010_93.
- 437 [22] V.M. Patel, B.G. Prajapati, M.M. Patel, Design and characterization of chitosan-containing
 438 mucoadhesive buccal patches of propranolol hydrochloride, *Acta Pharm. Zagreb Croat.* 57 (2007) 61–
 439 72. <https://doi.org/10.2478/v10007-007-0005-9>.
- 440 [23] A. Kaur, G. Kaur, Mucoadhesive buccal patches based on interpolymer complexes of chitosan-pectin
 441 for delivery of carvedilol, *Saudi Pharm. J. SPJ Off. Publ. Saudi Pharm. Soc.* 20 (2012) 21–27.
 442 <https://doi.org/10.1016/j.jsps.2011.04.005>.
- 443 [24] E.M. Varoni, L. Altomare, A. Cochis, A. GhalayaniEsfahani, A. Cigada, L. Rimondini, L. De Nardo,
 444 Hierarchic micro-patterned porous scaffolds via electrochemical replica-deposition enhance neo-
 445 vascularization, *Biomedical Materials Accepted* (2016).
- 446 [25] L. Bonetti, A. Caprioglio, N. Bono, G. Candiani, L. Altomare, Mucoadhesive chitosan-methylcellulose
 447 oral patches for the treatment of local mouth bacterial infections, *Biomater. Sci.* 11 (2023) 2699–
 448 2710. <https://doi.org/10.1039/d2bm01540d>.
- 449 [26] J. Xu, S. Strandman, J.X.X. Zhu, J. Barralet, M. Cerruti, Genipin-crosslinked catechol-chitosan
 450 mucoadhesive hydrogels for buccal drug delivery, *Biomaterials* 37 (2015) 395–404.
 451 <https://doi.org/10.1016/j.biomaterials.2014.10.024>.
- 452 [27] A. Ghalayani Esfahani, L. Altomare, E.M. Varoni, S. Bertoldi, S. Farè, L. De Nardo, Electrophoretic
 453 bottom up design of chitosan patches for topical drug delivery, *J. Mater. Sci. Mater. Med.* 30 (2019)
 454 40. <https://doi.org/10.1007/s10856-019-6242-x>.
- 455 [28] E.A. Kharenko, N.I. Larionova, N.B. Demina, Mucoadhesive Drug Delivery Systems: Quantitative
 456 Assessment of Interaction Between Synthetic and Natural Polymer Films and Mucosa, *Pharm. Chem.*
 457 *J.* 42 (2008) 392–399. <https://doi.org/10.1007/s11094-008-0132-8>.
- 458 [29] H. Yuk, C.E. Varela, C.S. Nabzyk, X. Mao, R.F. Padera, E.T. Roche, X. Zhao, Dry double-sided tape for
 459 adhesion of wet tissues and devices, *Nature* 575 (2019) 169–174. <https://doi.org/10.1038/s41586-019-1710-5>.
- 460 [30] Varoni, E, Vijayakumar, S, E. Canciani, A. Cochis, L. De Nardo, G. Lodi, L. Rimondini, M. Cerruti,
 461 Chitosan-Based Trilayer Scaffold for Multi-Tissue Periodontal Regeneration, *J. Dent. Res.* (2017).
 462 <https://doi.org/10.1177/0022034517736255>.
- 463 [31] S. Martinotti, M. Patrone, M. Manfredi, F. Gosetti, M. Pedrazzi, E. Marengo, E. Ranzato, HMGB1
 464 Osteo-Modulatory Action on Osteosarcoma SaOS-2 Cell Line: An Integrated Study From Biochemical
 465 and -Omics Approaches, *J. Cell. Biochem.* 117 (2016) 2559–2569. <https://doi.org/10.1002/jcb.25549>.
- 466 [32] M. Manfredi, S. Martinotti, F. Gosetti, E. Ranzato, E. Marengo, The secretome signature of malignant
 467 mesothelioma cell lines, *J. Proteomics* 145 (2016) 3–10. <https://doi.org/10.1016/j.jprot.2016.02.021>.

- 469 [33] L. Bonetti, A. Caprioglio, N. Bono, G. Candiani, L. Altomare, Mucoadhesive chitosan–methylcellulose
470 oral patches for the treatment of local mouth bacterial infections, *Biomater. Sci.* 11 (2023) 2699–
471 2710. <https://doi.org/10.1039/D2BM01540D>.
- 472 [34] Y. Zhou, M. Wang, C. Yan, H. Liu, D.-G. Yu, Advances in the Application of Electrospun Drug-Loaded
473 Nanofibers in the Treatment of Oral Ulcers, *Biomolecules* 12 (2022) 1254.
474 <https://doi.org/10.3390/biom12091254>.
- 475 [35] R.M. Gilhotra, M. Ikram, S. Srivastava, N. Gilhotra, A clinical perspective on mucoadhesive buccal drug
476 delivery systems, *J. Biomed. Res.* 28 (2014) 81–97. <https://doi.org/10.7555/JBR.27.20120136>.
- 477 [36] K.H. Clitherow, C. Murdoch, S.G. Spain, A.M. Handler, H.E. Colley, M.B. Stie, H. Mørck Nielsen, C.
478 Janfelt, P.V. Hatton, J. Jacobsen, Mucoadhesive Electrospun Patch Delivery of Lidocaine to the Oral
479 Mucosa and Investigation of Spatial Distribution in a Tissue Using MALDI-Mass Spectrometry Imaging,
480 *Mol. Pharm.* 16 (2019) 3948–3956. <https://doi.org/10.1021/acs.molpharmaceut.9b00535>.
- 481 [37] W. Samprasit, R. Kaomongkolgit, M. Sukma, T. Rojanarata, T. Ngawhirunpat, P. Opanasopit,
482 Mucoadhesive electrospun chitosan-based nanofibre mats for dental caries prevention, *Carbohydr.*
483 *Polym.* 117 (2015) 933–940. <https://doi.org/10.1016/j.carbpol.2014.10.026>.
- 484 [38] R. Shen, W. Xu, Y. Xue, L. Chen, H. Ye, E. Zhong, Z. Ye, J. Gao, Y. Yan, The use of chitosan/PLA nano-
485 fibers by emulsion eletrospinning for periodontal tissue engineering, *Artif. Cells Nanomedicine*
486 *Biotechnol.* 46 (2018) 419–430. <https://doi.org/10.1080/21691401.2018.1458233>.
- 487 [39] S. Mansuri, P. Kesharwani, K. Jain, R.K. Tekade, N.K. Jain, Mucoadhesion: A promising approach in
488 drug delivery system, *React. Funct. Polym. C* (2016) 151–172.
489 <https://doi.org/10.1016/j.reactfunctpolym.2016.01.011>.
- 490 [40] K. Mokabari, M. Iriti, E.M. Varoni, Mucoadhesive Vaccine Delivery Systems for the Oral Mucosa, *J.*
491 *Dent. Res.* 102 (2023) 709–718. <https://doi.org/10.1177/00220345231164111>.
- 492 [41] L.B. Hansen, L.L. Christrup, H. Bundgaard, Enhanced delivery of ketobemidone through porcine buccal
493 mucosa in vitro via more lipophilic ester prodrugs, *Int. J. Pharm.* 88 (1992) 237–242.
494 [https://doi.org/10.1016/0378-5173\(92\)90321-R](https://doi.org/10.1016/0378-5173(92)90321-R).
- 495 [42] L. Serpe, A. Jain, C.G. de Macedo, M.C. Volpato, F.C. Groppo, H.S. Gill, M. Franz-Montan, Influence of
496 salivary washout on drug delivery to the oral cavity using coated microneedles: An in vitro evaluation,
497 *Eur. J. Pharm. Sci. Off. J. Eur. Fed. Pharm. Sci.* 93 (2016) 215–223.
498 <https://doi.org/10.1016/j.ejps.2016.08.023>.
- 499 [43] S. Kumar, M. Prasad, R. Rao, Topical delivery of clobetasol propionate loaded nanosponge hydrogel
500 for effective treatment of psoriasis: Formulation, physicochemical characterization, antipsoriatic
501 potential and biochemical estimation, *Mater. Sci. Eng. C Mater. Biol. Appl.* 119 (2021) 111605.
502 <https://doi.org/10.1016/j.msec.2020.111605>.
- 503 [44] R. Panonnummal, R. Jayakumar, M. Sabitha, Comparative anti-psoriatic efficacy studies of clobetasol
504 loaded chitin nanogel and marketed cream, *Eur. J. Pharm. Sci. Off. J. Eur. Fed. Pharm. Sci.* 96 (2017)
505 193–206. <https://doi.org/10.1016/j.ejps.2016.09.007>.
- 506 [45] E. Marxen, M.D. Mosgaard, A.M.L. Pedersen, J. Jacobsen, Mucin dispersions as a model for the
507 oromucosal mucus layer in in vitro and ex vivo buccal permeability studies of small molecules, *Eur. J.*
508 *Pharm. Biopharm. Off. J. Arbeitsgemeinschaft Pharm. Verfahrenstechnik EV* 121 (2017) 121–128.
509 <https://doi.org/10.1016/j.ejpb.2017.09.016>.
- 510 [46] G.J.K. Praefcke, Regulation of innate immune functions by guanylate-binding proteins, *Int. J. Med.*
511 *Microbiol. IJMM* 308 (2018) 237–245. <https://doi.org/10.1016/j.ijmm.2017.10.013>.
- 512 [47] D.R. Adams, D. Ron, P.A. Kiely, RACK1, A multifaceted scaffolding protein: Structure and function, *Cell*
513 *Commun. Signal.* 9 (2011) 22. <https://doi.org/10.1186/1478-811X-9-22>.
- 514 [48] E. Buoso, M. Galasso, M.M. Serafini, M. Ronfani, C. Lanni, E. Corsini, M. Racchi, Transcriptional
515 regulation of RACK1 and modulation of its expression: Role of steroid hormones and significance in
516 health and aging, *Cell. Signal.* 35 (2017) 264–271. <https://doi.org/10.1016/j.cellsig.2017.02.010>.
- 517 [49] T. Calandra, T. Roger, Macrophage migration inhibitory factor: a regulator of innate immunity, *Nat.*
518 *Rev. Immunol.* 3 (2003) 791–800. <https://doi.org/10.1038/nri1200>.
- 519

Journal Pre-proof

521 **Figure legends**

522 **Figure 1. EPD apparatus and CS-CP patches' morphology.** Image of the EPD apparatus (A), used to obtain CS-
523 CP patches (B). Optical image of bilayer CS patch (C); optical image of bilayer CS-CP patch as (D).

524 **Figure 2. Morphology of the patches at scanning electron microscope (SEM).** (A and B) Bilayer CS patches
525 (bottom view and cross-section); (C and D) Bilayer CS-CP patches (top side view of the surface towards the
526 cathode, and cross-section); (E and F) Bilayer CS-CP patches before and after washing with PBS and ethanol
527 (top side view of the surface towards the solution): microspheres were ascribable to CP deposits (E), which
528 could be easily washed (F).

529 **Figure 3. Swelling behaviour of CS patches (green line) and of CS-CP patches (blue line),** up to 3 h after the
530 immersion in PSB solution at pH 7.4.

531 **Figure 4. CP release kinetics** from bilayer CS-CP patches, at *in vitro* test (PBS solution) (A-C) and *ex vivo* model
532 of porcine oral mucosa (D-F).

533 **Figure 5. Cytocompatibility of the patches and bioactivity of released CP.** (A) Metabolic activity (Alamar
534 Blue) of 3D model of oral mucosa in contact with bilayer CS patches versus CS-CP patches, showing no
535 significant difference in terms of cytocompatibility. (B) Map of the down/up-regulated protein coding genes
536 and their interconnection. List of down-regulated (C) or up-regulated proteins (D) upon contact with CS-CP
537 patches vs CP patches used as controls.

538

539

540 **Tables**

541 **Table 1.** Macro-pore diameters of CS and CS-CP bilayer patches.

Type of patch	Mean \pm SD
Bilayer CS	1.2 \pm 0.3 mm
Bilayer CS-CP	1.2 \pm 0.5mm

542

543

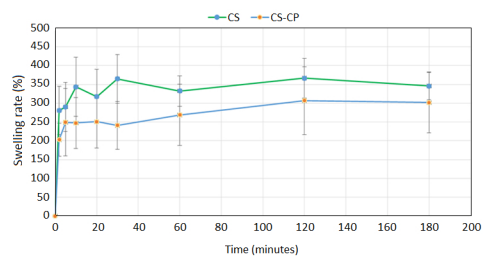
544 **Table 2.** Mucoadhesion test comparing CS (control) and CS-CP patches (test), expressed as release pressure
545 at detachment and muco-adhesion work.

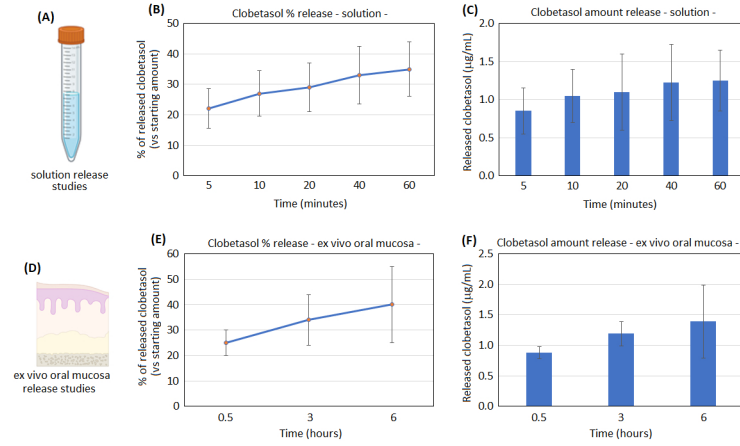
	CS	CS-CP
Release Pressure (Pa)	557.7±213.4	448.1±8.03
Work of adhesion (Pa*mm)	745.8±126.5	699.4±128.1

546

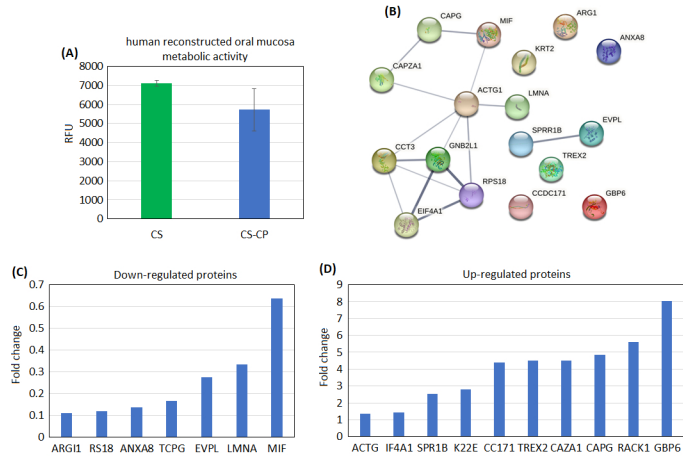
547

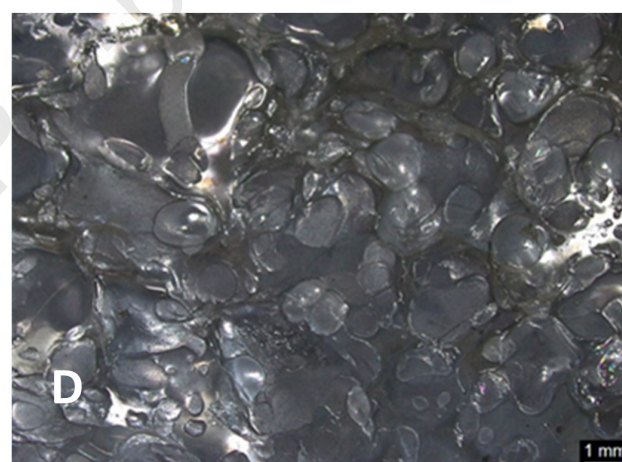
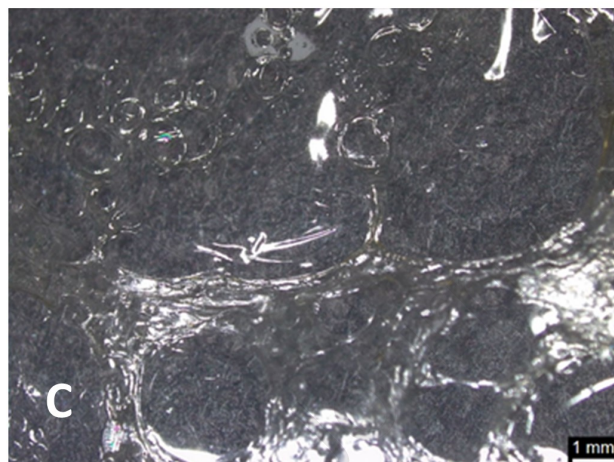
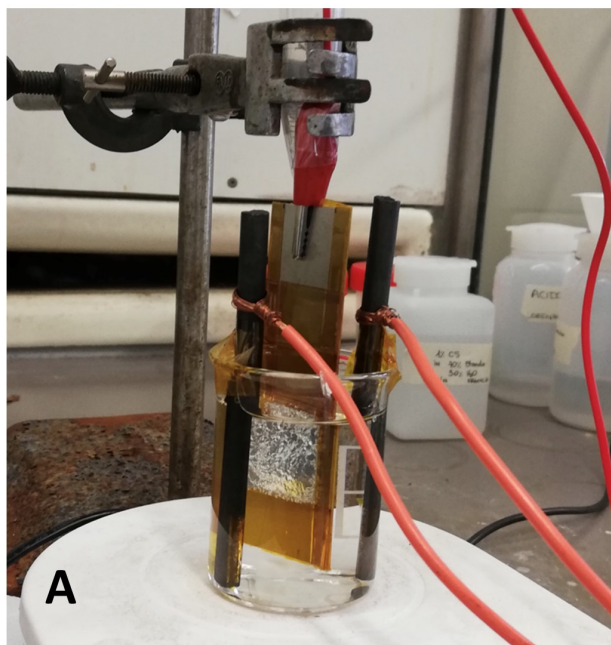
548

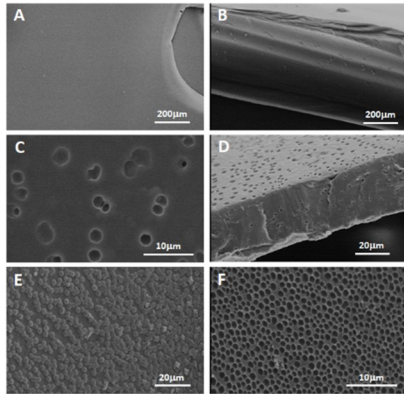




Journal Pre-proof







Journal Pre-proof

Highlights

- Highly lipophilic clobetasol propionate (CP) is successfully loaded on chitosan-based patches via electrophoretic deposition (EPD)
- Bilayer chitosan-based patches are promising mucoadhesive delivery systems for the oral cavity
- The presence of CP does not affect the mucoadhesive properties of chitosan-based patches
- CP, after the release from patches, maintains its biological immunosuppressive activity

Journal Pre-proof

Declaration of interests

The authors declare that they have no known competing financial interests or personal relationships that could have appeared to influence the work reported in this paper.

The authors declare the following financial interests/personal relationships which may be considered as potential competing interests:

Milan, 06/30/24

Elisa Maria Varoni